

Transport signature of pseudo-Jahn-Teller dynamics in a single-molecule transistor

F. RECKERMANN^{1,2}, M. LEIJNSE¹, M. R. WEGEWIJS^{1,2} and H. SCHOELLER¹

¹ *Institut für Theoretische Physik A, RWTH Aachen, 52056 Aachen, Germany*

² *Institut für Festkörper-Forschung - Theorie 3, Forschungszentrum Jülich, 52425 Jülich, Germany*

PACS 85.65.+h – Molecular electronic devices

PACS 71.70.Ej – Spin-orbit coupling, Zeeman and Stark splitting, Jahn-Teller effect

PACS 85.85.+j – Micro- and nano-electromechanical systems (MEMS/NEMS) and devices

Abstract. - We calculate the electronic transport through a molecular dimer, in which an excess electron is delocalized over equivalent monomers, which can be locally distorted. In this system the Born-Oppenheimer approximation breaks down resulting in quantum entanglement of the mechanical and electronic motion. We show that pseudo Jahn-Teller (pJT) dynamics of the molecule gives rise to conductance peaks that indicate this violation. Their magnitude, sign and position sharply depend on the electro-mechanical properties of the molecule, which can be varied in recently developed three-terminal junctions with mechanical control. The predicted effect depends crucially on the degree of intramolecular delocalization of the excess electron, a parameter which is also of fundamental importance in physical chemistry.

Introduction. - Nano-electromechanical devices (NEMS) electrically detect and control mechanical motion with great precision [1] and can be constructed in various nanostructures, including macromolecules such as suspended carbon nanotubes [2, 3]. Nowadays even nanometer sized molecules are within reach of experimental investigation. Successful three-terminal transport measurements [4] have been reported, detecting the quantized vibrational [5, 6], spin [7] and magnetic [8, 9] excitations of a single molecule. Quantum limited operation of NEMS is thus a starting point, rather than a goal in the single-molecule regime. More challenging is achieving control over such devices. Recently, electrical three-terminal devices have been demonstrated with additional mechanical control [10, 11]. Here the size of the nanogap in which the molecule is embedded can be adjusted with sub-Ångstrom precision, thereby changing the capacitive and resistive coupling of the molecule to the source and drain electrodes, as well as the intrinsic molecular properties. The interesting question arises how single-molecule quantum states involving electronic and mechanical degrees of freedom may be detected and controlled in such transport experiments. This has been addressed in several theoretical studies, e.g. [12–15]. Fundamental to nearly all of these works is the adiabatic Born-Oppenheimer (BO) approximation, where one separates the timescales of the fast

electronic motion from the slow dynamics of the nuclei. The transport is then governed by the Franck-Condon (FC) principle, where the tunneling of an electron onto the molecule changes the electron number $N \rightarrow N + 1$, which induces a transition between electronic states $e \rightarrow e'$ and the initial vibrational state χ_e is projected onto a vibrational state $\chi'_{e'}$ of the molecule in the final electronic state. The amplitude for this process factorizes and is proportional to the overlap integrals of the mechanical wave-functions $\langle \chi_e | \chi'_{e'} \rangle$ which in general is non-zero and strongly depends on both of the vibrational states. There are thus no selection rules in contrast to spin-related tunneling. By proper choice and design of the vibrational properties of molecular transistors (number of modes, adiabatic potential landscapes, etc.), the FC-effect may thus be exploited to induce non-trivial vibrational states and interesting non-linear transport characteristics relevant for possible electro-mechanical sensing applications. A novel aspect of molecule-based NEMS is they may display strong *vibronic* effects (distinct from vibrational) due to the non-trivial coupled quantum dynamics of the electronic and nuclear degrees of freedom, for a review see [16]. Here the Born-Oppenheimer separation of the time-scales for the nuclear and electron motion breaks down. The system is only adequately described by so-called vibronic states, in which the quantum entanglement renders the

concept of electronic and nuclear motion meaningless. The most prominent and well studied vibronic effect is the *dynamical* Jahn-Teller (JT) effect, which occurs in molecules where the electronic ground state is degenerate due to a high spatial symmetry of the static nuclear framework of the (non-linear) molecule. In such systems, there always exists [17] a vibrational coordinate along which a static distortion will lower the molecular symmetry and lift the degeneracy. However, in a single molecule, the distortions are dynamical and the electronic degeneracy is transformed into a vibronic degeneracy i.e. of the quantum-mechanical *molecular* eigenstates. Recently, the selection rules encoded in these molecular eigenstates (related to the high symmetry) were predicted to block electron transport through a JT active molecule [18]. An important question now is how to distinguish such vibronic blockade from spin- [19], magnetic [20] or Franck-Condon [14, 21, 22] blockade effects. Another issue is that the BO-approximation breaks down even when electronic levels only come close in energy (on the order of a few vibrational energy spacings). This is referred to as the dynamical *pseudo Jahn-Teller* effect and occurs in many molecular systems [16]. A generic problem where it occurs is in determining the degree of delocalization of an excess electron in a molecular dimer [23], which is fundamental to the classification of mixed-valence compounds by the Robin-Day (RD) scheme in physical chemistry. Dimers have also been considered in a transport setup [24–26] motivated by experiments [6].

In this Letter, we predict transport signatures of the pJT dynamics of a single molecular dimer transistor, which markedly differ from those due to the Franck-Condon effect, allowing the breakdown of the Born-Oppenheimer principle to be identified experimentally. We find characteristic non-linear conductance peaks with a sharp dependence of their *position, magnitude and sign* on the electro-mechanical parameters of the molecule.

Model. – We consider a dimer molecule consisting of two identical monomers, labelled by $i = 1, 2$, which can vibrate along their totally symmetric (“breathing”) mode Q_i about the potential minimum at $Q_i = 0$ with frequency ω . Each monomer accommodates one electronic orbital state, $|i\sigma\rangle$, for an excess electron with spin projection σ that can tunnel between the two monomers with amplitude t via a mechanically stiff bridging ligand. It thereby significantly distorts the occupied monomer along coordinate Q_i due to a change of the bond-lengths (c.f. Fig. 1(a)). The resulting shift of the potential minimum is $\sqrt{2}\lambda$, expressed in units of the zero-point motion energy of the vibration of the undistorted monomers. Thus λ is the dimensionless electron-vibration coupling. This model applies, for example, to a mixed-valence molecule [23], where the monomers are metal-ions (zero spin) with a surrounding shell of ligand atoms. The local distortion of the monomer is dragged along by the electron and becomes delocalized over the dimer. This results in coherent electro-mechanical mo-

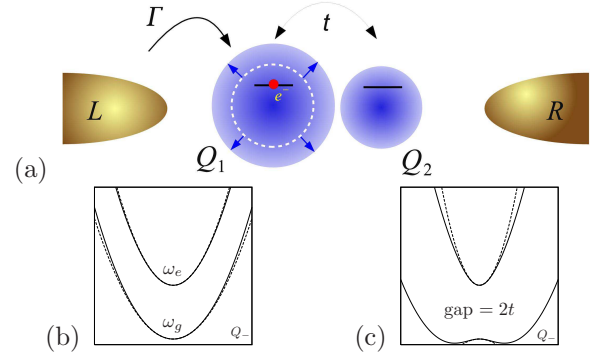


Fig. 1: (Color online) (a) Sketch: dimer molecule trapped in a nanogap between two voltage biased electrodes, $V_b = \mu_L - \mu_R$, and capacitively coupled to a back-gate (not shown) at voltage V_g , which shifts the effective molecular energy levels. The monomers (blue) can vibrate along the local totally symmetric breathing mode and are connected by a mechanically stiff bridge (not shown). (b-c) Adiabatic potentials W_g and W_e for the symmetry-breaking molecular distortion Q_- (full lines) and harmonic expansions around $Q_- = 0$ (dashed lines) for (b) weak ($\lambda = 0.7$, $t = 2.15\omega$) and (c) intermediate strength of the pJT effect ($\lambda = 1.93$, $t = 2.15\omega$).

tion and the breakdown of the Born-Oppenheimer separation. The central quantity controlling the character of the molecular states is the delocalization energy t relative to the coupling $\lambda\omega$ to the localized distortion. We note that in ref. [24], the opposite case of stiff monomers and a distorted bridge was considered, requiring only a single-mode to be considered, whereas here we account for two vibrational modes and their interplay. Also, below we consider transport up to high bias $V_b \sim 4t$, in contrast to [24, 25]. When the size of the nanogap is varied, for example in a mechanically controllable break-junction, the parameters ω , t and λ are expected to change, but not proportionally. Without loss of generality, we can assume that only the strength of the intramolecular hopping t changes while the mechanical properties, λ, ω , of the monomers remain fixed.

We assume charging effects (Coulomb blockade) to be strong enough that only two molecular charge states participate in transport processes, which we label by the number of excess electrons on the molecule $N = 0, 1$. The Hamiltonian H^N for the molecule in charge state N , written in the molecular vibrational coordinates $Q_{\pm} = (Q_2 \pm Q_1)/\sqrt{2}$, then reads

$$H^0 = \sum_{j=\pm} \frac{1}{2}\omega (P_j^2 + Q_j^2) \quad (1)$$

$$H^1 = H^0 - \lambda\omega Q_+ + \lambda\omega Q_- (\hat{n}_1 - \hat{n}_2) + t \sum_{\sigma} (d_{1\sigma}^{\dagger} d_{2\sigma} + h.c.) \quad (2)$$

where $d_{i\sigma}^{\dagger}$ creates an electron in state $|i\sigma\rangle$ and $\hat{n}_i = \sum_{\sigma} d_{i\sigma}^{\dagger} d_{i\sigma}$ is the occupation operator. The symmetric coordinate, Q_+ , corresponds to the monomer vibrating

in phase i.e. the *molecular* breathing mode where the molecule as a whole changes its size. It couples to the total excess charge, $\propto N$, of the molecule, resulting in a simple shift of the potential surface along Q_+ by an amount λ (linear term in eq. (2)). The Franck-Condon (FC) transport effects resulting from this type of coupling have been calculated by several groups [13–15, 21] and found experimentally [5, 6, 27]. In contrast, the anti-symmetric mode, Q_- , corresponds to the monomers vibrating with opposite phase. If an excess electron is present, this molecular shape distortion couples to the internal charge imbalance $\hat{n}_1 - \hat{n}_2$. Due to the intramolecular tunneling, t , the Hamiltonian (2) mixes electronic and vibrational states of the mode Q_- prohibiting a factorization of the molecular wave-function into a Q_- -vibrational and an electronic part. We thus need *vibronic* states, $|m_-, \sigma\rangle = |\chi_{m_-}^1\rangle|1\sigma\rangle + |\chi_{m_-}^2\rangle|2\sigma\rangle$, to describe the excess electron and the pJT-active mode. Here m_- denotes the vibronic quantum number for the joint electron-vibration (Q_-) system: distinguishing these systems is fundamentally impossible due to the quantum coherence. Finding the vibrational coefficients $|\chi_{m_-}^i\rangle$ in the molecular vibronic eigenstates requires diagonalization of the Hamiltonian (2), which has to be done numerically. Despite the breakdown of the BO-approximation, it is instructive to consider the adiabatic potentials for the Q_- vibrations, obtained by neglecting the nuclear kinetic energy operator ($P_- \rightarrow 0$) in eq. (2) and to find the electronic eigenstates as function of Q_- , while neglecting Q_+ . The resulting electronic energies are the ground (g) and excited (e) adiabatic Q_- -potential for the vibrations, $W_{g,e}(Q_-) = \frac{1}{2}\omega Q_-^2 \mp \sqrt{(\lambda\omega Q_-)^2 + t^2}$, which are sketched in fig. 1(b-c).

Transport. – The transport setup, sketched in fig. 1 (a), is described by the Hamiltonian $H = H_M + H_{\text{res}} + H_T$. Here the molecular part H_M is specified by $H^N + E_{\text{add}}(V_g)N$ for $N = 0, 1$ excess electrons where the gate voltage V_g effectively shifts the molecular energy levels by linearly changing the addition energy E_{add} . The electrodes $r = L, R$ are described by $H_{\text{res}} = \sum_{r,k,\sigma} (\epsilon_k - \mu_r) c_{rk\sigma}^\dagger c_{rk\sigma}$ and are kept at temperature T and electrochemical potentials $\mu_r = \mu \pm V_b/2$ i.e. V_b is the bias voltage. They are coupled to the molecule by $H_T = \sum_{r,i,k,\sigma} T_r^i d_{i\sigma}^\dagger c_{rk\sigma} + h.c.$, where $c_{rk\sigma}^\dagger$ creates an electron of spin σ in state k in electrode r and T_r^i is the amplitude for tunneling between the electrode r and monomer $i = 1, 2$. We consider a linear arrangement as sketched in fig. 1(a) by assuming $T_L^2 = T_R^1 = 0$ and, for simplicity, symmetric coupling $T_L^1 = T_R^2 = \sqrt{\Gamma}/(2\pi\rho)$. Here Γ denotes the tunneling rate and ρ is the electrode density of states. In many experiments [5–9, 27] the transport is dominated by single-electron tunneling. We therefore focus on the corresponding range of applied voltages and temperature. We calculate the non-equilibrium stationary state occupations of the molecular states and the transport current both up to second order in H_T

using a standard kinetic (master) equation, see e.g. [15].

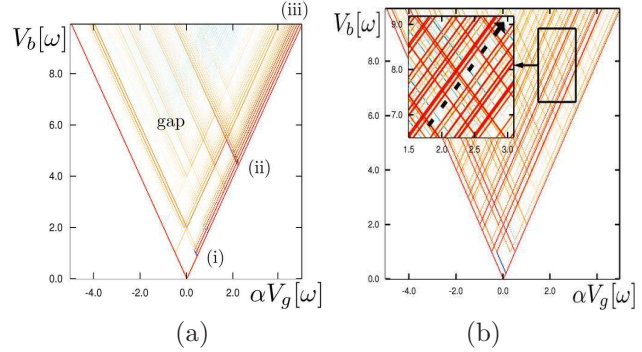


Fig. 2: (Color online) dI/dV_b ($\Gamma = 2.5 \cdot 10^{-5}\omega$, $T = 4 \cdot 10^{-3}\omega$) for (a) weak pJT mixing ($\lambda = 0.7$, $t = 2.15\omega$) (b) moderate pJT mixing ($\lambda = 1.93$, $t = 2.15\omega$). Inset: high contrast, dashed black line marking the $V_b - V_g$ trace taken in fig. 3(a). For convenience the gate voltage is defined such that $V_g = 0$ corresponds to the charge degeneracy point and $\alpha = dE_{\text{add}}/dV_g$. Due to symmetric biasing, energy scales appear at twice the separation on the voltage axis.

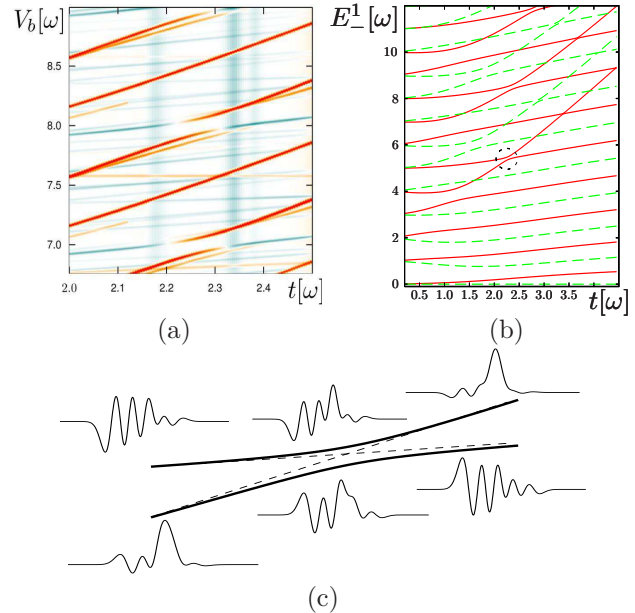


Fig. 3: (Color online) Signature of the pJT effect: anti-crossings as the intramolecular delocalization t is varied due to a mechanical change of the nanogap size. (a) Evolution with t of the dI/dV_b trace along the line in the V_b, V_g plane marked in the inset of fig. 2(b). (b) Evolution with t of energies of the vibronic states for $N = 1$ ($\lambda = 1.93$), with the harmonic Q_+ -vibration energies subtracted. For $t \sim \omega\lambda^2$, the level repulsion and the entanglement are most drastic. The green (dashed) / red (solid) color indicates positive / negative parity. The anti-crossing in the transport in (a) corresponds to the marked anti-crossing around $t \approx 2.3\omega$ and $E_-^1 \approx 5\omega$. (c) Evolution with t of the vibrational parts $\chi_{m_-}^1(Q_-)$. Due to the symmetry of the dimer, the vibronic state has definite molecular parity $\pi = \pm$, reflected by the property $\chi_{m_-}^1(Q_-) = \pi\chi_{m_-}^1(-Q_-)$.

Results. – In order to appreciate the breakdown of the BO separation, we first discuss a case where it has approximate validity i.e. the effect of the distortion of the monomers is sufficiently weak. In fig. 2(a) we show the differential conductance as function of the applied voltages. Many excitations appear, involving the Q_+ and/or the Q_- mode, which are separated in bias voltages by multiples of 2ω (due to symmetric biasing). The first of these excitations starts out at the marker (i) in fig. 2(a). However, in contrast to usual FC transport spectra [13–15], the Q_- excitations are suppressed within the noticeable gap of $4t$, and enhanced conductance peaks (starting out from marker (ii)) delimit the upper boundary of the gap. One can thus directly estimate the strength of the delocalization of the excess electron. Furthermore, the excitations spaced in V_b roughly by 2ω also have a detailed substructure of a dense series of conductance peaks, for instance, along the right edge of the transport region, terminating at the marker (iii). The latter correspond to tunnel processes between Q_- excitations of the $N = 0$ and $N = 1$ ground potential with the same vibrational quantum number $m_- = 0, 1, 2, \dots$. For $\lambda^2\omega \ll t$, the potential $W_g(Q_-)$ is approximately harmonic, but with reduced frequency $\omega_g/\omega \approx 1 - \omega\lambda^2/t$ due to the pJT interaction, see fig. 1(b). Therefore the resonances corresponding to different m_- occur at slightly different positions [15]. The equidistant energy spacings correspond to $\omega - \omega_g \approx (\lambda\omega)^2/t \ll \omega$. Similarly, above the gap near marker (ii), a dense series of conductance peaks with negative V_g dependence indicates that the upper adiabatic potential has a higher frequency $\omega_e/\omega = 1 + \omega\lambda^2/t$. Using the gap and features at (i)-(iii) in fig. 2(a) one can thus estimate λ , t and ω from the transport data. For larger values of λ , the adiabatic potentials additionally become an-harmonic due to the pJT interaction resulting in markedly non-equidistant spacing of the dense series of conductance peaks. We note that, interestingly, in mixed-valence molecules with magnetic ions this vibrational an-harmonicity correlates with the relative orientations of the ionic spins [28].

The most dramatic effect of the pJT interaction is the breakdown of the BO separation for stronger coupling λ . This occurs at high bias voltage $V_b \sim 4t$ i.e. above the gap where anti-crossings occur when *excited states* of the two adiabatic potentials W_e and W_g come close in energy. At a first glance, the transport spectrum in this case, shown in fig. 2(b), seems inextricably complex. However, clear signatures of the pJT effect are revealed when the nano-gap size is varied and the intramolecular hopping t changes while the mechanical properties of the monomers λ, ω remain fixed. In fig. 3(a) we show the evolution of the dI/dV_b trace taken along the dashed black line in the inset of fig. 2(b), as t is varied. Experimentally, such data can be collected with techniques described in [10,11]. The dI/dV_b resonances with a weak t -dependence one would assign to highly excited vibrations in the lower adiabatic

electronic state, W_g , whereas those with a strong linear t -dependence would correspond to the lowest excitations in the upper adiabatic electronic state, W_e . This distinction is completely lost at the anti-crossings visible in fig. 3(a). The conductance anti-crossing at $t \approx 2.3\omega$ maps out the corresponding anti-crossing in the evolution of the vibronic energy spectrum with t which is shown in fig. 3(b). Strikingly, the *sign* of the conductance of the two anti-crossing transport resonances is different. This directly relates to the large difference in the kinetic energy of the nuclear motion of the two anti-crossing adiabatic electronic states. In fig. 3(c) we show vibrational components of the vibronic wave-functions of the involved states. Far from the anti-crossing their spatial variation is clearly different, resulting in different transport rates and therefore non-equilibrium occupations and conductance. At the anti-crossing the strong pJT mixing causes the components of *both* vibronic wave-functions to rapidly vary. As a result the conductance peaks disappear in a narrow range of t values in the anti-crossing region. Note that all other resonances, which follow from the BO approximation and the FC-principle, smoothly depend on t , making the pJT effect clearly stand out. Strikingly, the transport anti-crossings seen in fig. 3(a) are *replicas* of one and the same anti-crossing marked in fig. 3(b), due to the simultaneous excitation of the Q_+ mode. Thus, interestingly, the *pJT-inactive mode* proliferates the violation of the adiabatic BO separation in the transport. The many other anti-crossings in fig. 3(b) result in pJT resonances at different voltages (not shown), and comparison with these calculated levels allows one to estimate the parameters. More generally, the effects exemplified above may be expected whenever the pJT mixing is important, that is, for minimal separation of the adiabatic potentials on the order of the vibrational quanta, $t \sim \omega$, and moderate to strong coupling to the distortion, $\lambda \gtrsim 1$.

Conclusion. – We have shown that the breakdown of the Born-Oppenheimer separation of the electronic and vibrational motion in a molecular transistor leads to novel pseudo Jahn-Teller transport resonances which can be distinguished from standard Franck-Condon effects. The combination of electrostatic gating and mechanical control is crucial to unravel such complex molecular transport processes and demonstrate electro-mechanical quantum entanglement in molecule-based NEMS. Interesting candidate devices are mixed valence molecules with a moderate degree of intramolecular delocalization of the excess electron, so-called Robin-Day Class II systems. Their electron transport properties may shed new light on the fundamental issue in physical chemistry of their classification by intramolecular charge transfer.

* * *

We acknowledge K. Flensberg for discussions and the financial support from DFG SPP-1243, the NanoSci-ERA,

the Helmholtz Foundation, the EU-RTN Spintronics, and the FZ-Jülich (IFMIT).

REFERENCES

- [1] EKINCI K. L. and ROUKES M. L., *Rev. Sci. Instrum.* , **76** (2005) 061101.
- [2] SAZONOVA V., YAISH Y., USTUNEL H., ROUNDY D., ARIAS T. A. and MCEUEN P. L., *Nature* , **431** (2004) 284.
- [3] SAPMAZ S., JARILLO-HERRERO P., BLANTER Y., DEKKER C. and VAN DER ZANT H. S. J., *Phys. Rev. Lett.* , **96** (2006) 026801.
- [4] PARK H., LIM A. K. L., ALIVISATOS A. P., PARK J. and MCEUEN P. L., *Appl. Phys. Lett.* , **75** (1999) 301.
- [5] PARK H., PARK J., LIM A. K. L., ANDERSON E. H., ALIVISATOS A. P. and MCEUEN P. L., *Nature* , **407** (2000) 52.
- [6] PASUPATHY A. N., PARK J., CHANG C., SOLDATOV A. V., LEBEDKIN S., BIALCZAK R. C., GROSE J. E., DONEV L. A. K., SETHNA J. P., RALPH D. C. and MCEUEN P. L., *Nano Lett.* , **5** (2005) 203.
- [7] OSORIO E. A., O'NEILL K., WEGEWIJS M. R., STUHR-HANSEN N., PAASKE J., BJØRNHOLM T. and VAN DER ZANT H. S., *Nano Lett.* , **7** (2007) 3336.
- [8] HEERSCHE H. B., DE GROOT Z., FOLK J. A., VAN DER ZANT H. S. J., ROMEIKE C., WEGEWIJS M. R., ZOBBI L., BARRECA D., TONDELLO E. and CORNIA A., *Phys. Rev. Lett.* , **96** (2006) 206801.
- [9] JO M.-H., GROSE J. E., BAHETI K., DESHMUKH M. M., SOKOL J. J., RUMBERGER E. M., HENDRICKSON D. N., LONG J. R., PARK H. and RALPH D. C., *Nano Lett.* , **6** (2006) 2014.
- [10] CHAMPAGNE A. R., PASUPATHY A. N. and RALPH D. C., *Nano Lett.* , **5** (2005) 305.
- [11] PARKS J. J., CHAMPAGNE A. R., HUTCHISON G. R., FLORES-TORRES S., ABRUÑA H. D. and RALPH D. C., *Phys. Rev. Lett.* , **99** (2007) .
- [12] FLENSBERG K., *Phys. Rev. B* , **68** (2003) 205324.
- [13] MITRA A., ALEINER I. and MILLIS A. J., *Phys. Rev. B* , **69** (2004) 245302.
- [14] KOCH J. and VON OPPEN F., *Phys. Rev. Lett.* , **94** (2005) 206804.
- [15] WEGEWIJS M. R. and NOWACK K. C., *New J. of Phys.* , **7** (2005) 239.
- [16] BERSUKER I. B. and POLINGER V. Z., *Vibronic interactions in molecules and crystals* (Springer) 1989.
- [17] JAHN H. A. and TELLER E., *Proc. Roy. Soc. London* , **161** (1937) 220.
- [18] SCHULTZ M. G., NUNNER T. S. and VON OPPEN F., *Berry-phase effects in transport through single jahn-teller molecules* cond-mat/0702489.
- [19] ROMEIKE C., WEGEWIJS M. R. and SCHOELLER H., *Phys. Rev. B* , **75** (2007) 064404.
- [20] ROMEIKE C., WEGEWIJS M. R. and SCHOELLER H., *Phys. Rev. Lett.* , **96** (2006) 196805.
- [21] BRAIG S. and FLENSBERG K., *Phys. Rev. B* , **68** (2003) 205324.
- [22] BRAIG S. and FLENSBERG K., *Phys. Rev. B* , **70** (2004) 085317.
- [23] BERSUKER I. and BORSHCH S., *Vibronic Interactions in Polynuclear Mixed-Valence Clusters* Vol. 81 of *Advances in Chemical Physics* (Wiley) 1992 Ch. 6 p. 703.
- [24] KAAT G. A. and FLENSBERG K., *Phys. Rev. B* , **71** (2005) 155408.
- [25] DONARINI A., GRIFONI M. and RICHTER K., *Phys. Rev. Lett.* , **97** (2006) 166801.
- [26] CHANG C. T., SETHNA J. P., PASUPATHY A. N., PARK J., RALPH D. and MCEUEN P., *Phys. Rev. B* , **76** (2007) 045435.
- [27] OSORIO E. A., O'NEILL K., STUHR-HANSEN N., NIELSEN O. F., BJØRNHOLM T. and VAN DER ZANT H. S., *Adv. Mater.* , **19** (2007) 281.
- [28] RECKERMANN F., LEIJNSE M., WEGEWIJS M. R. and SCHOELLER H., submitted.